Polymerization and Membrane Characteristics of Aqueous Bilayers of Glutamate-Based Double-Chain Ammonium Amphiphiles[1]

Toyoki Kunitake,* Naotoshi Nakashima,[2] and Masashi Kunitake[2]

Department of Organic Synthesis, Faculty of Engineering, Kyushu University, Fukuoka 812, Japan. *Received October 5, 1988; Revised Manuscript Received December 28, 1988*

ABSTRACT: A series of monoacryl and diacryl double-chain ammonium amphiphiles were synthesized and their bilayer characteristics before and after photopolymerization were examined. UV irradiation of unpolymerized bilayer dispersions in water gave polymerized bilayers without much change in the aggregation number, although the morphologies of the latter as observed by negative-staining electron microscopy were less ordered than those of the former. The molecular weight of the polymers in organic solvents amounted to several millions. Diacrylated bilayers gave large fractions of the insoluble product upon polymerization. The molecular organization in the polymerized bilayer was scrutinized by a combination of thermal and spectral measurements. Differential scanning calorimetry showed that sharp phase transitions observed in the unpolymerized bilayers became broader and were accompanied by hysteresis upon polymerization. The benzene unit in the spacer portion of a polymerizable amphiphile was a versatile internal probe for assessing the bilayer alignment. The much enhanced circular dichroism of the unpolymerized, crystalline bilayer was reduced and displayed large hysteresis upon polymerization. Strong fluorescence emission from the benzene unit was observed in the crystalline bilayers. Fluorescence recovery after rapid cooling and absorption spectral equilibration of a membrane-bound cyanine dye were also slow in the polymer. A certain degree of disordering in the molecular alignment remained for bilayers polymerized in the liquid-crystalline state.

Introduction

Polymerized bilayer membranes or polymer vesicles have been investigated actively in the past several years.[3,4] The most important aspect of these studies is covalent reinforcement of the bilayer membrane that is basically formed by noncovalent self-assemblage of component molecules. Polymerization was expected to lead to stabilization of vesicular morphologies and to improve barrier capacities against permeation of ions and molecules, thus facilitating their use in drug delivery and related functions.

Polymerization can, on the other hand, disturb the bilayer organization and cause deterioration of the membrane characteristics. In the past examples, the barrier property has not necessarily been improved by polymerization. It is highly desirable at this time to carry out a systematic examination of the influence of polymerization on the bilayer characteristics.

It has been pointed out that the physical characteristics, especially the phase transition behavior, of a polymerized bilayer membrane are critically affected by the location of the polymerizable unit in a molecule.[5] Polymerization of the terminal vinyl group in the alkyl chain lowers the gel-to-liquid crystal phase transition temperature (T_c),[6] and polymerization of the diacetylene unit in the middle of the alkyl chain causes disappearance of the phase transition.[7,8] In contrast, polymerization at the hydrophilic head group does not produce much change in T_c and is apparently better for preserving the bilayer characteristics.[9-11] Examples of polymerizable groups in this class of compounds include the methacrylate unit,[12] the styrene unit,[10,11] and the allyl unit[13,14] bonded to the polar head of dialkylammonium salts. The methacrylate unit was also introduced to the ammonium site of a phosphocholine amphiphile.[9] Neumann and Ringsdorf reported that peptide formation at the polar head slightly lowered the T_c.[15] In other cases, the polymerizable group is introduced as counterions of charged, double-chain amphiphiles.[16,17] Polymeric bilayers that are obtained by copolymerization of hydrophilic monomers and double-chain monomers were shown to maintain the typical membrane characteristics,[18] and the presence of hydrophilic spacer groups between the polymer chain and the amphiphilic side chain efficiently decoupled the motion of these two portions.[19]

Chart I

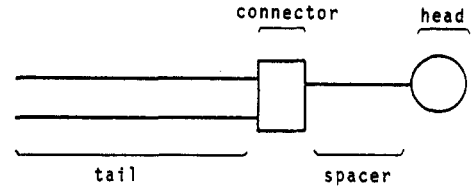

A large variety of synthetic amphiphiles form stable bilayer membranes upon dispersion in water, and double-chain amphiphiles are representative bilayer-forming compounds. Their general structure is composed of flexible tails, connector, spacer, and hydrophilic head, as shown in Chart I. The glutamic acid unit is superior as connector, and dialkyl glutamate amphiphiles gave well-developed bilayer structures with sharper phase-transition behavior when compared with simple dialkylammonium salts.[20] Therefore, we have prepared a large number of dialkyl glutamate derivatives as reference compounds. In this paper, we introduce the acrylate unit in the hydrophilic portion of dialkyl glutamate derived ammonium amphiphiles and examine their bilayer characteristics before and after polymerization.

The structures of the amphiphiles used in this study and their abbreviations are given in Chart II. Compounds **1–4** are polymerizable double-chain amphiphiles with different combinations of tail and spacer. The methylene tail, C_m, is mainly related to packing stability, and the chain lengths of C_{12}–C_{16} are most typical of bilayer-forming amphiphiles. The spacer methylene, C_n, plays a crucial role in controlling molecular orientation and morphology. The two spacers C_2 and C_{11} are extremes in length. The molecular orientation in bilayer assembly can be monitored through spectroscopic changes of covalently and noncovalently bound chromophores.[21,22] The benzene unit in compound **5** is introduced to monitor the change in molecular orientation upon polymerization. Compound **6** is used to see if cross-linking is possible at the membrane surface.

Experimental Section

Materials. Polymerizable amphiphiles were synthesized by quaternization of double-chain precursors with acrylates. The preparation of the ω-halo precursors was briefly described else-

0024-9297/89/2222-3544$01.50/0

Chart II

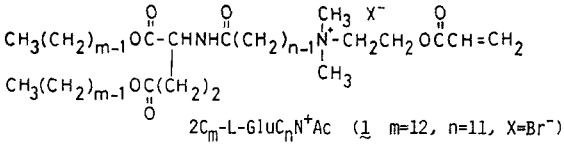

$2C_m$-L-Glu$C_n N^+$Ac (1 m=12, n=11, X=Br^-)
(2 m=14, n=2, X=Cl^-)
(3 m=14, n=11, X=Br^-)
(4 m=16, n=11, X=Br^-)

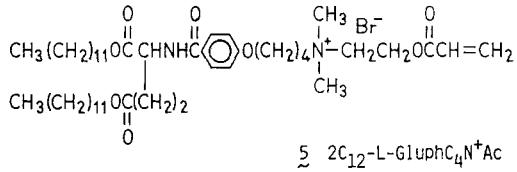

5 $2C_{12}$-L-GluphC$_4N^+$Ac

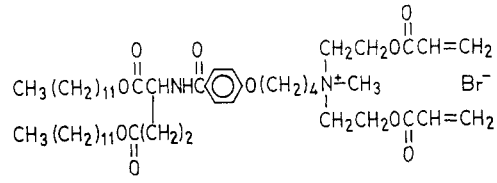

6 $2C_{12}$-L-GluphC$_4N^+$2Ac

where.[21] In a representative procedure, 2.5 g (3.4×10^{-3} mol) of didodecyl *N*-(11-bromoundecanoyl)-L-glutamate and 5 g (3.5×10^{-2} mol) of 2-(dimethylamino)ethyl acrylate (Kojin Co., bp 79 °C (30 mmHg)) were dissolved in a dried 1:1 (v/v) mixture of tetrahydrofuran (THF) and acetonitrile and stirred for 1 week at room temperature in the dark. A spatula full of dibutylhydroxytoluene was added as a polymerization inhibitor. Solvent was removed from the reaction mixture and the solid residue was recrystallized twice from ethyl acetate to give colorless powders of **1** in 77% yield: mp 28→44 °C (the arrow indicates the presence of the liquid-crystalline region); ^{1}H NMR ($CDCl_3$) δ 1.4–1.8 (m, 64 H), 2.1–2.4 (m, 5 H), 3.2–3.7 (N^+CH_2, N^+CH_3, s + t, 10 H), 3.9–4.3 (OCH_2, m, 6 H), 5.8–6.5 (vinyl, 3 H); IR (Nujol, cm^{-1}) 1455 ($\nu_{C=O}$, ester), 1380 (amide). Anal. Calcd for $C_{47}H_{89}O_7N_2Br \cdot 0.5H_2O$: C, 63.92; H, 10.27; N, 3.17. Found: C, 63.77; H, 10.20; N, 3.22.

The other acrylate amphiphiles were quaternized by essentially the same procedure.

2: yield 58%; mp 32→109 °C; ^{1}H NMR ($CDCl_3$) δ 0.9–1.5 (m, 56 H), 2.1–2.7 (m, 5 H), 3.6 (s, N^+CH_3, 6 H), 3.7–4.3 (m, 9 H), 5.7–6.4 (vinyl, 3 H); IR (Nujol, cm^{-1}) 3100 (ν_{NH}), 1730 ($\nu_{C=O}$, ester), 1660 ($\nu_{C=O}$, amide). Anal. Calcd for $C_{42}H_{79}O_7N_2Cl$: C, 66.42; H, 10.48; N, 3.69. Found: C, 64.57; H, 10.50; N, 3.72.

3: yield 78%; mp 30–48 °C; ^{1}H NMR ($CDCl_3$) δ 0.9–1.8 (m, 72 H), 2.1–2.4 (m, 5 H), 3.2–3.7 (m, N^+CH_3, N^+CH_2, 10 H), 3.9–4.3 (m, OCH_2, 6 H), 5.8–6.5 (vinyl, 3 H); IR (Nujol, cm^{-1}) 1735 ($\nu_{C=O}$, ester), 1670 ($\nu_{C=O}$, amide). Anal. Calcd for $C_{51}H_{97}O_7N_2Br \cdot 0.5H_2O$: C, 65.22; H, 10.52; N, 2.98. Found: C, 65.29; H, 10.44; N, 3.09.

4: yield 56%; mp room temp→84 °C. Anal. Calcd for $C_{55}H_{105}O_7N_2Br$: C, 66.97; H, 10.73; N, 2.84. Found: C, 66.68; H, 11.01, N, 2.88.

5: yield 58%; mp 37→123 °C; ^{1}H NMR ($CDCl_3$) δ 0.8–2.3 (m, 52 H), 2.3–2.9 (m, 7 H), 3.3–3.9 (m, 6 H), 4.0–4.5 (m, OCH_2, 6 H), 5.9–6.6 (vinyl, 3 H), 6.9–8.3 (Ar and NH, 5 H); IR (Nujol, cm^{-1}) 1730 ($\nu_{C=O}$, ester), 1630 ($\nu_{C=O}$, amide). Anal. Calcd for $C_{47}H_{81}O_8N_2Br \cdot 1.5H_2O$: C, 62.10; H, 9.31; N, 3.08. Found: C, 62.18; H, 9.14; N, 3.23.

Methylbis(acryloxyethyl)amine was obtained by slowly adding a THF solution of 2.5 equiv of freshly distilled acryl chloride and a small amount of dibutylhydroxytoluene into a stirred THF solution of *N*-methyldiethanolamine (Wako, 1st grade) and 2.5 equiv of triethylamine with ice cooling. The precipitate of triethylamine hydrochloride was removed and THF was distilled off in vacuo. The oily product was purified by distillation and identified by IR and NMR spectroscopy: yield 54%; bp 106–108 °C (0.33 mmHg).

Methylbis(acryloxyethyl)amine (5 g, 4.3×10^{-2} mol) and 3 g (4.2×10^{-3} mol) of the bromide precurser were allowed to react in the presence of dibutylhydroxytoluene in 100 mL of dry CH_3CN at 40–50 °C in the dark for 1 week. Solvent was removed and the solid residue was recrystallized twice from ethyl acetate: **6**, colorless powder, yield 43%; mp 38→118 °C; ^{1}H NMR ($CDCl_3$) δ 0.8–2.1 (m, 52 H), 2.2–2.5 (m, 3 H), 3.45 (s, N^+CH_3, 3 H), 3.8–4.9 (m, 16 H), 5.7–6.5 (vinyl, 6 H), 6.7–8.0 (Ar, 4 H); IR (Nujol, cm^{-1}) 1730 ($\nu_{C=O}$, ester), 1620 ($\nu_{C=O}$, amide), 970 (vinyl). Anal. Calcd for $C_{51}H_{85}O_{10}N_2Br \cdot H_2O$: C, 62.24; H, 8.91; N, 2.85. Found: C, 61.99; H, 8.90; N, 2.86.

Polymerization. Weighed amounts of the polymerizable amphiphiles were added to deionized water, swollen at 60–70 °C and sonicated for ca. 1 min by a Branson 185 cell disruptor to obtain 20 mM dispersions. Nitrogen gas was bubbled into the dispersions for 30 min and the solutions were irradiated at given temperatures (a water-jacketed holder was used) for 10 or 20 min at a fixed distance of 30 cm with a ultrahigh-pressure Hg lamp (Ushio high-pressure Hg Lamp UI-501C, 250 W). No filters were used. Water was then removed in vacuo. The residual polymer was dissolved in $CDCl_3$ and disappearance of the vinyl proton was confirmed by ^{1}H NMR spectroscopy (Hitachi R-600).

Measurements. Aggregate weights of monomeric and polymeric bilayers were measured with low-angle laser light scattering (instrument, Toyosoda LS-8). The samples were dissolved in deionized water, and a series of monodisperse poly(ethylene oxides) were used for calibration. The molecular weight of individual polymers was measured in THF or in $CHCl_3$, and monodisperse polystyrenes were used for calibration.

Aggregate morphology was examined by transmission electron microscopy (Hitachi H-600). In the case of unpolymerized aggregates, powder samples were dispersed by sonication in 2% aqueous uranyl acetate, and dispersions (20 mM) were spotted on carbon-coated copper meshes and air-dried. In the case of polymerized aggregates, 20 mM dispersions of polymers were mixed with equal volumes of 2% aqueous uranyl acetate and sonicated, and the mixtures were spotted on Cu meshes. The polymerization in the presence of uranyl acetate produced ill-characterized precipitates.

Dark-field optical microscopy (Olympus BH-2) was also used for examination of aggregate morphology. Powder samples (1 mg) were added to 1 mL of deionized water, sonicated, and allowed to stand for 1 week at 5–10 °C. Transparent dispersions thus obtained were placed on slide glasses and observed at room temperature (20–25 °C).

The phase transition behavior was studied with a differential scanning calorimeter (instrument, Seiko Instruments SSC/560). Aqueous dispersions (20 mM) were prepared by sonication and the measurement was repeated between 0 to 80 °C at a heating rate of 2 °C/min. ΔH was obtained from peak areas by the base-line method and ΔS was determined by dividing ΔH by the peak top temperature (in kelvin). The detailed procedure is given elsewhere.[20] Circular dichroism (CD) spectra were obtained with a JASCO J40AS spectropolarimeter. The aqueous samples (0.1 mM) were incubated for several days at 5–10 °C, and the spectral change with elevating temperature was recorded. Fluorescence spectra were obtained with a Hitachi fluorescence spectrophotometer, Model 650–60. Rhodamine B was used as quantum counter. The sample solutions used in CD measurements were transferred to a 1-cm quartz cell for fluorescence measurements. An identical solution was used in alternation for CD and fluorescence measurements in the case of temperature change. The excitation wavelength was set at 260 nm, where the benzene ring absorbs.

Dye Binding. Aqueous bilayer aggregates (2.5×10^{-4} M) were placed in a UV cell, and small amounts of a trimethine cyanine dye in ethanol were injected (the final dye concentration, 5.0×10^{-6} M). Absorption spectra of these dye/bilayer solutions were measured with a Hitachi spectrophotometer 220A.

Results and Discussion

Polymerization. Polymerizations were conducted by photoirradiation of aqueous bilayer dispersions. Their turbidities were not detectably enhanced upon polymerization: the dispersions remained translucent. Although the unpolymerized dispersions were often transformed into swollen gels after standing for long periods of time, the polymerized bilayer dispersions remained stable even after

Table I
Aggregate Weight of Unpolymerized and Polymerized Bilayers and Molecular Weight of Polymerized Amphiphiles

amphiphile	polymerizatn condtns: °C, min	aggregate wt in water × 10^{-6}	molec wt ($\overline{DP}$)[a] in THF or $CHCl_3$ × 10^{-6}
$2C_{14}$-L-$GluC_2N^+Ac$	unpolymerized	16	
(2) (T_c, 29 °C)	20, 10		0.14 (180)
	40, 10	21	0.51 (670)
$2C_{14}$-L-$GluC_{11}N^+Ac$	20, 10		0.063 (68)
(3) (T_c, 43 °C)	20, 20		0.81 (870)
	30, 10		0.24 (260)
	40, 10		0.41 (440)
	50, 10		1.1 (1200)
$2C_{16}$-L-$GluC_{11}N^+Ac$	unpolymerized	25	
(4) (T_c, 47 °C)	30, 10		0.18 (260)
	60, 10	25	4.6 (4700)
$2C_{12}$-L-$GluphC_4N^+Ac$	unpolymerized	130	
(5) (T_c, 32 °C)	20, 10		0.075 (82)
	40, 10	110	2.5 (2700)
$2C_{12}$-L-$GluphC_4N^+2Ac$	40, 10		2.6 (2600)
(6) (T_c, 24 °C)			
5/6 (mole ratio, 9/1)	40, 10		9.1 (9900)

[a] Degree of polymerization.

several months. Similarly enhanced stabilities have been reported in other studies. No precipitates were formed from polymerized dispersions of diacrylated bilayer **6**.

Table I gives molecular weights of aqueous dispersions (aggregate weight) and of polymers. The molecular weights of the unpolymerized dispersions are in the range (10–10^2) × 10^6, as are typical of the bilayer aggregate. These values are virtually unchanged after polymerization for the three cases examined. The polymerization, therefore, proceeds within the aggregate and does not appreciably change the aggregation number.[23]

The molecular weights of the polymers were subsequently measured in good solvents such as $CHCl_3$ and THF, in which polymers are supposed to be molecularly dissolved. They are in the range (0.1–5) × 10^6 for the monoacryl bilayers. These values are close to those reported by Ringsdorf and co-workers for bilayers of **7** that were polymerized by a water-soluble azo initiator.[12] Molecular weights have been rarely included in the published papers on polymerized vesicles.

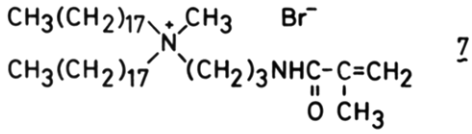

7

In the case of the $2C_{14}GluC_{11}N^+Ac$ (**3**) bilayer, polymerization was carried out at 20, 30, 40, and 50 °C. Under otherwise similar conditions, the molecular weight increases with rising temperature, and the increase is particularly noticeable at 50 °C. This jump appears to reflect the change in the physical state of the membrane, since phase transition as determined by DSC occurs at 42 °C. Similar jumps of molecular weight are found for other bilayers, $2C_{12}GluC_2N^+Ac$ (**2**), $2C_{16}GluC_{11}N^+Ac$ (**4**), and $2C_{12}GluphC_4N^+Ac$ (**5**), at polymerization temperatures above T_c. It is often assumed that polymerization is facilitated in the bilayer assembly, as monomers are juxtaposed in two dimensions. This does not necessarily hold true. Although the observed degrees of polymerization are never too small, the presumably fixed spatial arrangement of the acrylate unit at the crystalline membrane surface is not particularly favorable for radical propagation. Enhanced fluidity of the liquid-crystalline bilayer leads to a much higher molecular weight. To our knowledge, the influence of the physical state of the membrane on the polymerization behavior was reported only by Regen and co-workers.[17] They conducted photopolymerization of dioctadecyldimethylammonium methacrylate and found that poly(methacrylate) obtained at $T < T_c$ contained larger amounts of the isotactic and heterotactic triads than that obtained at $T > T_c$.

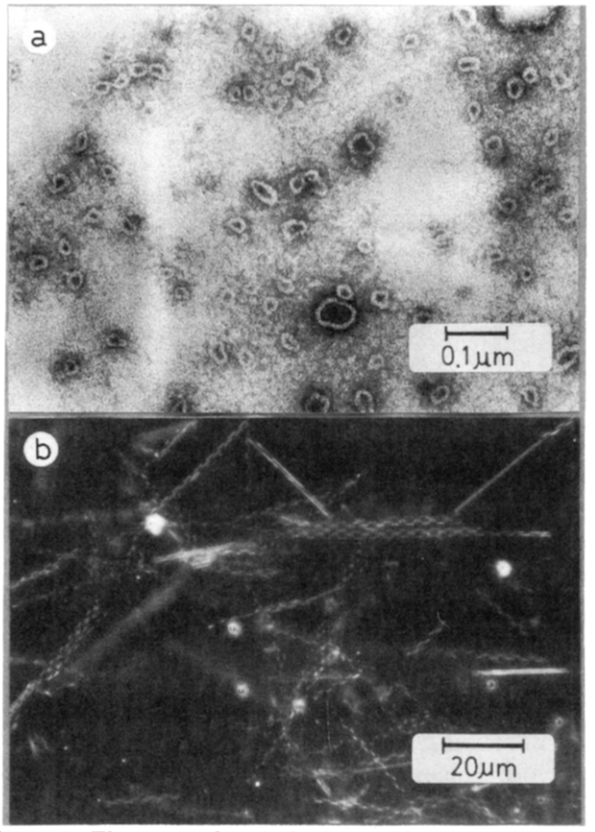

Figure 1. Electron and optical micrographs of unpolymerized bilayer of **1**. (a) electron micrograph, stained by uranyl acetate, original magnification × 80000; (b) dark-field optical micrograph, sample 1 mM, aged for 1 month at room temperature, original magnification ×800.

Polymerization of diacrylate **6** led to a significant amount of the $CHCl_3$-insoluble fraction. The molecular weight of the $CHCl_3$-soluble fraction was not very high.

The increase in molecular weight due to involvement of the diacrylate monomer is apparent in the polymerization of mixed monomers. A 9:1 (mol/mol) mixture of **5** and **6** gave the highest molecular weight of 9.1 × 10^6. The $CHCl_3$-insoluble fraction was not present. This molecular weight implies that a typical bilayer aggregate is composed of about *ten* polymer molecules. Although cross-linking at the diacrylate monomer unit must occur, it is not frequent enough to produce insoluble polymers at this molar ratio.

Electron and Light Microscopy. Amphiphile **1** gives typical bilayer vesicles upon sonication in water as shown by the electron micrograph in Figure 1. Single-walled vesicles with layer thickness of 80 Å and diameter of 300–1000 Å are found abundantly. In dark-field light microscopy, these aggregates are seen as spherical objects shortly after dispersion. They are transformed into regular helices when allowed to stand at room temperature for 1 month (Figure 1b). Helix formation needs a much longer time compared with the corresponding nonpolymerizable amphiphile **8**, which produced similar helices in 1 week.[26] When the vesicular dispersion was photoirradiated (40 °C, 10 min), electron microscopy indicated the presence of the bilayer structure but the vesicles were less clearly seen. Photoirradiation of the helical dispersion also led to its

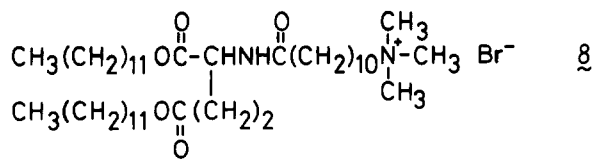

8

destruction. These results clearly show that polymerization interferes with the formation of highly regular bilayers.

Formation of bilayer vesicles and lamellar aggregates was also observed for other amphiphiles of Chart II. Polymerization by photoirradiation produced less-ordered bilayer aggregates.

Differential Scanning Calorimetry. The gel-to-liquid crystal phase transition is one of the fundamental properties of the bilayer membrane. The existence of the phase transition is a strong indication of the bilayer structure and the membrane fluidity is largely determined by phase transition.

Figure 2 shows DSC thermograms of aqueous bilayers of 1 before and after polymerization. The unpolymerized dispersion gives a sharp peak at 29 °C. The first DSC scan after polymerization displays a less sharp peak at the same temperature; however, repeated scans produce broader, multiplet peaks. The phase transition temperatures (T_c, DSC peak top) and the corresponding ΔH and ΔS values obtained in this study are summarized in Table II. The phase transition was observed in all cases except for the polymer of 6.[27] Therefore, polymerization does not intrinsically destroy the bilayer structure. This is probably because the acrylate units are present at the hydrophilic portion. Other workers have used bilayer membranes that are polymerizable at the hydrophilic head and concluded that the phase transition due to bilayer assembly is maintained after polymerization (see below).[9-12,19] However, Regen et al. recently introduced a thiol unit at the connector end of the alkyl chain and found that disulfide formation did not appreciably lower T_c.[21,28,29]

The following additional conclusions are derived from the DSC data.

(a) The spacer methylene length affects phase transitions of *unpolymerized* bilayers. We have made an extensive survey of the effect of spacer methylene length on the phase transition behavior.[20] T_c is either elevated, lowered, or unchanged with changing spacer lengths, depending on the connector structure. When the glutamate unit is used as connector, T_c is elevated with increasing spacer lengths. Incorporation of the benzene unit in the spacer also raises T_c. The same conclusion is reached here by a comparison of **2**, **3**, and **5**.

(b) Polymerization affects the phase transition behavior to different degrees, depending on the monomer structure and the polymerization conditions. When the spacer methylene is short (compound **2**), polymerization (at 20 °C) raises T_c by ca. 6 deg. Repeated scans give analogous thermograms. Polymerization at a higher temperature (40 °C) gives T_c close to that of the unpolymerized **2**. Apparently, the bilayer physical state (gel versus liquid crystal) during polymerization affects the molecular organization of the resulting polymeric bilayer.

(c) When the spacer methylene is longer, as in **3**, polymerization causes larger changes. In polymerization at temperatures below T_c, the DSC peak becomes broadened after the second scan, whereas the thermogram is quite broad even from the first scan for this bilayer, which is polymerized at 40 °C.

(d) When the benzene unit is included in the spacer portion as in **5**, the DSC behavior of the polymerized bilayer is very close to that of the unpolymerized counterpart. The T_c value is also unmodified by polymerization when 10 mol % of bisacryl component **6** is introduced.

(e) The polymerization temperature causes DSC peak broadening to different degrees. In the polymerization at temperatures below T_c of the unpolymerized bilayer, DSC peaks are as sharp as those of the unpolymerized ones at least in the first scan. The subsequent scans give broader peaks. The original side-chain packing is apparently not readily recovered. Partially disordered molecular packing is fixed when the polymerization proceeds in the liquid-crystalline bilayer, since DSC peaks are broad from the first scan in this case.

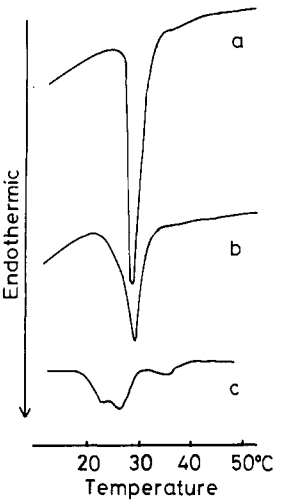

Figure 2. DSC Thermograms of 1, 20 mM aqueous dispersion: (a) unpolymerized sample; (b) after photopolymerization at 20 °C for 10 min, first scan; (c) the second scan of the polymerized sample.

Table II
Phase Transition of Unpolymerized and Polymerized Bilayers

aqueous bilayer	polymerizatn condtns: °C, min	molec wt × 10^{-6}	T_c, °C	ΔH kJ/mol	ΔS,[a] J/K·mol
1	unpolymerized		28.8	42	139
	20, 10		29.0	14	47
			34.7	9	28
	40, 10		27.0	13	43
2	unpolymerized		28.1	21	71
	20, 20	0.14	34.8	20	63
			34.7[b]	9	28
	40, 10	0.51	27.0	13	43
3	unpolymerized		41.8	42	133
	20, 20	0.81	44.1	42	134
	30, 10		43.6	17	53
	40, 10	0.41	40.0	20	63
	50, 10	1.1	40.0	10	31
5	unpolymerized		32.2	58	188
	40, 10	2.5	28.5	31	102
6	unpolymerized		23.5	51	172
	40, 10	2.6		no peak	
5/6 (9:1)	unpolymerized		28.6	52	172
	40, 10	9.1	29.0	21	69

[a] $\Delta H/T$ for sharp peaks. [b] The second scan.

Spectroscopic Characteristics. The molecular organization as inferred from the DSC behavior is manifest in many cases in the spectroscopic properties. We have frequently used absorption and emission spectra and circular dichroism in order to delineate the molecular organization of bilayers. As discussed in the Introduction, the benzene chromophore in the spacer portion is a powerful spectral probe for this purpose.

For the aqueous bilayer of 8,[21] circular dichroism (CD) is much enhanced at temperatures below T_c: $[\theta]_{max} > 10^5$. The enhancement is totally lost ($[\theta]$ ca. 6000), as the bilayer

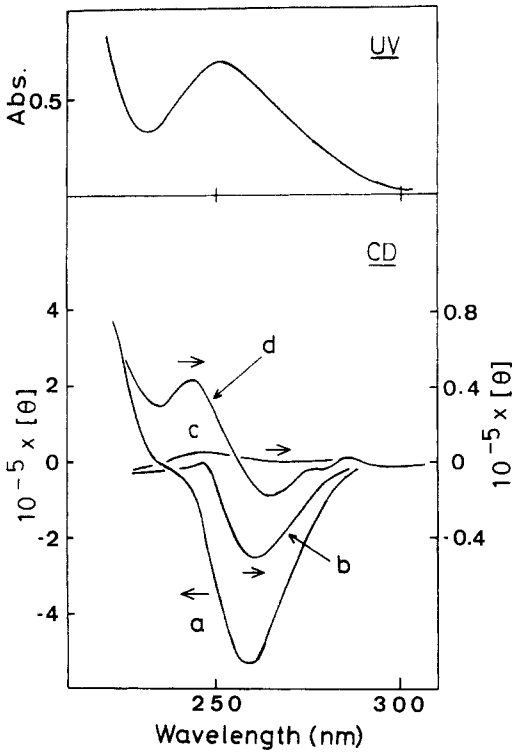

Figure 3. UV and CD spectra of aqueous bilayer of **5**, 1.0×10^{-4} M: (a) unpolymerized sample, CD measurement at $T < T_c$; (b) after photopolymerization at 20 °C for 10 min and the subsequent aging at 15 °C for 2 weeks; (c) unpolymerized and polymerized samples, CD measurement at $T > T_c$; (d) after photopolymerization at 40 °C for 10 min, CD measurement at 15 °C.

undergoes phase transition to the liquid-crystalline state. It is clear that the CD enhancement arises from strong dipole coupling of spatially fixed chromophores in the crystalline state. In the same vein, monomeric emission (λ_{max} 320 nm) is observed for the crystalline bilayer, but excimer emission is found at $T > T_c$.[30]

The bilayer of **5** gives identical absorption spectra, typical of the benzene unit, before and after polymerization (Figure 3). In contrast, the CD spectrum is strongly influenced by polymerization. The unpolymerized bilayer displays a negative Cotton effect with $[\theta]_{max}$(260 nm) of -5×10^5 (curve a), which however, is lost in the liquid-crystalline bilayer (curve c). The original enhancement is recovered by allowing the sample to stand for a few days at 20 °C. The recovery is extremely slow at lower temperatures. These results are almost identical with those observed for the bilayer of the corresponding trimethylammonium amphiphile **9**, although the spectral hysteresis is greater in the former. The identical CD enhancement implies that the presence of the acryloylethyl group in place of the methyl group at the head position does not alter the molecular packing.

The bilayer sample that is polymerized at $T < T_c$ gives a multiply coupled spectrum similar to that of the unpolymerized bilayer but with ca. 10% intensity: $[\theta]_{max}$ −50000 at 270 nm (curve b). This intensity was attainable by aging of the polymerized bilayer dispersion for 2 weeks at 15 °C. Additional small enhancements are found by further aging. The bilayer that was polymerized at 40 °C (above T_c) gives also a reduced spectrum with a positive $[\theta]_{max}$ of $+4.6 \times 10^4$ at 240 nm. This spectrum is similar in shape and intensity to that observed for a rapidly cooled unpolymerized sample from $T > T_c$. The polymerization in the liquid-crystalline state apparently fixes disordered chromophore arrangements similar to that obtained by the liquid-crystalline state of the unpolymerized bilayer.

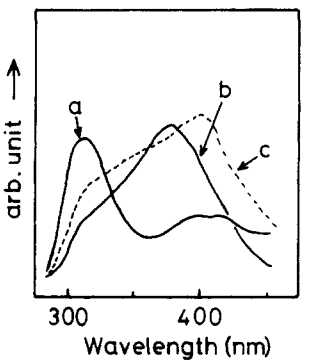

Figure 4. Corrected emission spectra of bilayer of **5**, sample 0.1 mM, excitation at 260 nm: (a) unpolymerized bilayer, measurement at 10 °C; (b) photopolymerized (at 40 °C for 10 min) bilayer; (c) the unpolymerized sample was rapidly cooled to 10 °C from a temperature above T_c.

Fluorescence spectra were measured for the same samples as employed for the CD measurement. As shown in Figure 4, the unpolymerized bilayer at $T < T_c$ gives the monomeric emission at 320 nm with a smaller excimer component at 410 nm. Upon raising the temperature of measurement, the "excimer" component is intensified at the expense of the monomer component near the phase transition temperature. When the sample was rapidly cooled from a temperature above T_c, the excimer spectrum did not change even after prolonged aging (curve c). Apparently, the structural disorder introduced by the quenching cannot be remedied. This result shows a very good correspondence to the lack of the CD recovery for a rapidly cooled sample from a temperature above T_c. The polymer sample (polymerized at 20 °C) gives a broad emission with a maximum at 410 nm (excimer peak) and a shoulder at 300–350 nm (monomer peak), similar to curve c. This indicates that the bilayer is partially disordered. On the other hand, a broad emission centered at 380 nm together with a small shoulder at 300–350 nm is observed at 5–40 °C for the sample polymerized at 40 °C (curve b). The emission intensity is enhanced with lowering the temperature, but the spectral shape does not change. The emission maximum at 380 nm is located at the midpoint between the monomer emission (λ_{max} 320 nm) and the excimer emission (λ_{max} 410 nm) of the unpolymerized bilayer. Therefore the polymerization in the liquid-crystalline state seems to fix an emission site which is composed of the neighboring chromophores in a different arrangement. This arrangement is not critically affected by the phase transition (T_c 29 °C). Again, this emission characteristic corresponds very nicely to the CD data.

Dye Binding. Negatively charged cyanine dyes are efficiently bound to ammonium bilayer membranes, and their spectra change characteristically due to specific dye–membrane interactions. Cyanine dye NK 2012 displays particularly marked spectral changes so that it is a useful probe for the structure of the bilayer surface.[31]

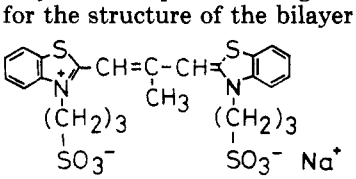

Cyanine dye NK 2012

Figure 5 (curve a) is an absorption spectrum of the cyanine dye bound to the unpolymerized bilayer of **5** at room temperature (below T_c). A sharp peak found at 570 nm is typical of the J-aggregated dye. The major peak is slowly intensified and a shoulder at 500 nm that is at-

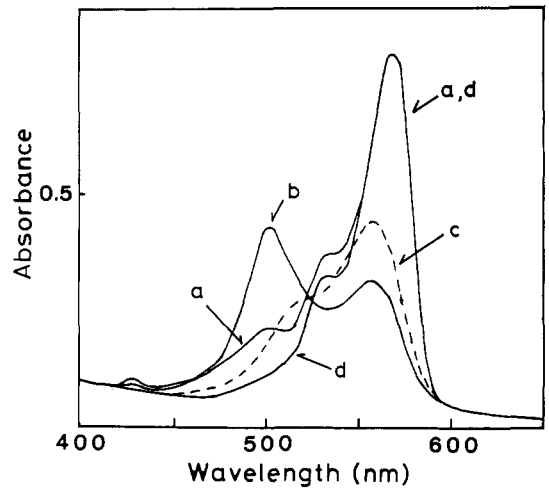

Figure 5. Absorption spectra of a membrane-bound cyanine dye, dye (NK 2012) 5.0×10^{-6} M, bilayer 5 2.5×10^{-4} M: (a) unpolymerized bilayer, measurement at 15 °C; (b) photopolymerized (at 40 °C for 10 min) bilayer, measurement at 15 °C; (c) polymerized and unpolymerized bilayers, measurement at 55 °C (above T_c); (d) polymerized sample after aging at 55 °C, measurement at 15 °C.

tributable to the card-packed dye (the H aggregate) is lessened accordingly. When the temperature of measurement is raised beyond T_c, this sharp peak is replaced with a broad peak at 560 nm (curve c). The latter spectrum is typically seen for the "monomeric" dye bound to liquid-crystalline bilayers. The original spectrum is regenerated by lowering the temperature. These temperature-dependent changes are very similar to those observed with the trimethylammonium bilayer of **9**. However, a

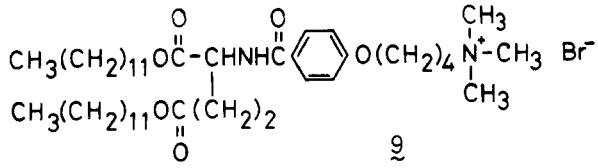

9

remarkable difference exists in the binding behavior between these two bilayers. The spectral change of NK 2012 due to binding and association at the bilayer surface of **9** is complete in a matter of minutes, whereas several hours are required for the spectral equilibration on the unpolymerized bilayer of **5**. It appears that the acryloylethyl group at the membrane surface interferes with the positional readjustment of the bound dye molecules. This must be related to a slow recovery of the CD intensity of the unpolymerized bilayer at lowered temperatures. We may be able to make bilayer organization of extremely strong hysteresis by introducing appropriate head groups.

When the anionic dye is added to a polymerized bilayer at 15 °C, two maxima are found at 500 nm and at 560 nm, as shown in Figure 5 (curve b). They are attributed to the H aggregate and the monomeric species, respectively. As the temperature is raised beyond T_C (55 °C in this case), the broad peak at 560 nm becomes predominant (curve c). When the temperature is again lowered to 15 °C, the spectrum turns to that of the J aggregate (curve d).

These situations are schematically illustrated in Figure 6. The cyanine dye produces the J aggregate as the most stable form on the unpolymerized and polymerized bilayer. However, the acryloyl unit and its polymer at the membrane surface slow down formation of this aggregate; the latter to a much greater degree. Therefore, when the dye is added to the polymerized bilayer, it first forms the H aggregates without much specific interaction with the ammonium bilayer (Figure 6a). The dye is dispersed much

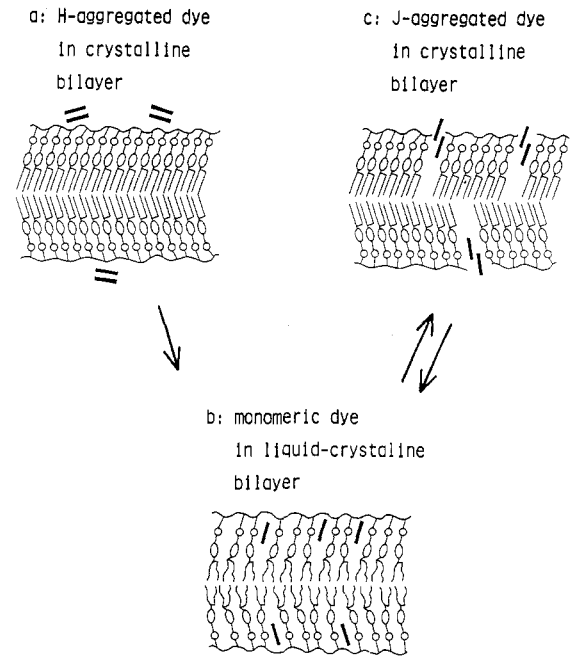

Figure 6. Schematic illustrations of the mode of dye binding.

better in the liquid-crystalline bilayer (Figure 6b), and the molecularly dispersed dye molecules can produce more favorable J aggregates once the membrane is transformed to the crystalline phase (Figure 6c).

Concluding Remarks

We have shown in this study how polymerization at the hydrophilic head region affects the component alignment in the bilayer, on the basis of several physicochemical measurements. Major conclusions obtained are as follows:

(1) The phase transition temperatures of unpolymerized bilayers do not shift much upon polymerization, if the bilayers are incubated sufficiently. However, the polymerized bilayers showed DSC peak broadening and much stronger hysteresis. The bilayers polymerized in the crystalline state gave sharp peaks in the first scan, similar to those of the unpolymerized bilayer. The peaks are much broader in the subsequent scans. Broad DSC peaks are found from the first scan for bilayers polymerized in the liquid-crystalline state. Therefore, it is clear that realignment of the side chain does not proceed smoothly in the case of polymerized bilayers. The different DSC behavior arising from the change in the physical state during polymerization is interesting. Since the difference cannot be eliminated by incubation, there may be a difference in molecular structure between polymers obtained in the crystalline and liquid-crystalline states. Regen and coworkers[32] reported that the main-chain tacticity of the polymerized bilayer is uniquely affected by the polymerization temperature. Therefore, the change in the extent of side-chain alignment during polymerization may cause differences in the main-chain stereochemistry. This can lead to a permanent difference in the DSC behavior.

(2) The benzene unit in the spacer portion is a versatile spectroscopic probe for assessing the bilayer organization. The CD and emission spectra reflect the bilayer organization sensitively. These data also indicate that the bilayer polymerized in the crystalline state is better organized than that polymerized in the liquid-crystalline state. Large hysteresis was found for these spectra of polymerized bilayers.

(3) Absorption spectra of a membrane-bound cyanine similarly reflect the extent of organization of the polymerized bilayer. As illustrated in Figure 6, the favored form

of dye aggregation (J aggregate) on the polymerized bilayer cannot be accomplished directly. It is possible only after the dye is dispersed monomerically in the liquid-crystalline bilayer. Therefore, the polymer main-chain interferes with free reorganization of bound dye molecules. This result suggests an interesting possibility. The main-chain interference in combination with large hysteresis of the side-chain alignment would create widely variable (nonuniform) binding sites at the membrane surface. A synthetic analogue of antibody formation may be envisaged by using the present results.

Registry No. 1, 120712-49-4; 1 (homopolymer), 120712-55-2; 2, 120712-50-7; 2 (homopolymer), 120712-56-3; 3, 120712-51-8; 3 (homopolymer), 120712-57-4; 4, 120712-52-9; 4 (homopolymer), 120712-58-5; 5, 120712-53-0; 5 (homopolymer), 120712-59-6; 6, 120712-54-1; 6 (homopolymer), 120712-60-9; NK 2012, 17701-26-7.

References and Notes

(1) Contribution no. 892 from the Department of Organic Synthesis.
(2) Present address: Department of Industrial Chemistry, Faculty of Engineering, Nagasaki University, Nagasaki 852, Japan.
(3) Fendler, J. H. *Membrane Mimetic Chemistry*; Wiley–Interscience: New York, 1982; p 492–505.
(4) Ringsdorf, H.; Schlarb, B.; Venzmer, J. *Angew. Chem., Int. Ed. Engl.* **1988**, *27*, 113–158.
(5) Akimoto, A.; Dorn, K.; Gros, L.; Ringsdorf, H.; Schupp, H. *Angew. Chem., Int. Ed. Engl.* **1981**, *20*, 90–91.
(6) Regen, S. L.; Czech, B.; Singh, A. *J. Am. Chem. Soc.* **1980**, *102*, 6638–6640.
(7) Ringsdorf, H.; Schupp, H. *Makromol. Chem.* **1981**, *182*, 247–253.
(8) Leaver, J.; Alonso, A.; Durrani, A.; Chapman, D. *Biochim. Biophys. Acta.* **1983**, *732*, 210–218.
(9) Kusumi, A.; Singh, M.; Tirrell, D. A.; Oehme, G.; Singh, A. Samuel, N. K. P.; Hyde, J.; Regen, S. L. *J. Am. Chem. Soc.* **1983**, *105*, 2975–2980.
(10) Reed, W.; Guterman, L.; Tundo, P.; Fendler, J. H. *J. Am. Chem. Soc.* **1984**, *106*, 1897–1907.
(11) Nome, F.; Reed, W.; Politi, M.; Tundo, P.; Fender, J. H. *J. Am. Chem. Soc.* **1984**, *106*, 8086–8093.
(12) Dorn, K.; Klingbiel, R. T.; Specht, D. P.; Tyminsky, P. N.; Ringsdorf, H.; O'Brien, D. F. *J. Am. Chem. Soc.* **1984**, *106*, 1627–1633.
(13) Babilis, D.; Dais, P.; Margaritis, L. H.; Paleos, C. M. *J. Polym. Sci., Polym. Chem. Ed.* **1985**, *23*, 1089–1098.
(14) Iino, Y.; Ogata, Y.; Shigehara, K.; Tsuchida, E. *Makromol. Chem.* **1985**, *186*, 923–931.
(15) Neumann, R.; Ringsdorf, H. *J. Am. Chem. Soc.* **1986**, *108*, 487–490.
(16) Aliev, K. V.; Ringsdorf, H. Schlarb, B.; Leister, K. H. *Makromol. Chem., Rapid Commun.* **1984**, *5*, 345–352.
(17) Fukuda, H.; Diem, T.; Stefely, J.; Kezdy, F. J.; Regen, S. L. *J. Am. Chem. Soc.* **1986**, *108*, 2321–2327.
(18) Kunitake, T.; Nakashima, N.; Takarabe, K.; Nagai, N.; Tsuge, A.; Yanagi, H. *J. Am. Chem. Soc.* **1981**, *103*, 5945–5947.
(19) Elbert, R.; Laschewsky, A.; Ringsdorf, H. *J. Am. Chem. Soc.* **1985**, *107*, 4134–4141.
(20) Kunitake, T.; Ando, R.; Ishikawa, Y. *Mem. Fac. Eng., Kyushu Univ.* **1986**, *46*, 221–243.
(21) Kunitake, T.; Nakashima, N.; Shimomura, M.; Okahata, Y.; Kano, K.; Ogawa, T. *J. Am. Chem. Soc.* **1980**, *102*, 6642–6644.
(22) Nakashima, N.; Fukushima, H.; Kunitake, T. *Chem. Lett.* **1981**, 1207–1210.
(23) A reviewer pointed out that molecular weights determined in $CHCl_3$ or THF are likely to be artificially high due to polymer aggregation via charge clustering. We therefore determined molecular weight of an analogous polymer sample ($2C_{16}$-L-$GluC_2N^+Ac$, $\bar{M}_n$ 4.6×10^6) by gel permeation chromatography in $CHCl_3$. This technique uses lower polymer concentrations compared with low-angle laser light scattering. The measurements conducted at two different concentrations (by 5-fold) and in the absence and presence of tetrabutylammonium bromide (which eliminates polymer aggregation[24,25]) gave virtually the same result. Therefore, we conclude that the molecular weight data obtained in organic solvents (Table I) are free of aggregation.
(24) Dorn, K.; Patton, E. V.; Klingbiel, R. T.; O'Brien, D. F.; Ringsdorf, H. *Makromol. Chem., Rapid Commun.* **1983**, *4*, 513–517.
(25) Bolikal, D.; Regen, S. L. *Macromolecules* **1984**, *17*, 1287–1289.
(26) Nakashima, N.; Asakuma, S.; Kim, J.; Kunitake, T. *Chem. Lett.* **1984**, *10*, 1709–1712.
(27) DSC measurement was made directly for an aqueous dispersion of **6** after photoirradiation. The dried polymer sample contained $CHCl_3$-soluble and $CHCl_3$-insoluble fractions; however, even the $CHCl_3$-soluble fraction could not be redispersed in water. It appears that extensive, three-dimensional crosslinking occurred during solvent removal and modified organized bilayer structures.
(28) Regen, S. L.; Yamaguchi, K.; Samuel, N. K. P.; Singh, A. *J. Am. Chem. Soc.* **1983**, *105*, 6354–6355.
(29) Samuel, N. K. P.; Singh, M.; Yamaguchi, K.; Regen, S. L. *J. Am. Chem. Soc.* **1985**, *107*, 42–47.
(30) Kunitake, T.; Tawaki, S.; Nakashima, N. *Bull. Chem. Soc. Jpn.* **1983**, *56*, 3235–3242.
(31) Nakashima, N.; Tsuge, A.; Kunitake, T. *J. Chem. Soc., Chem. Commun.* **1985**, 41–42.
(32) Regen, S. L.; Samuel, N. K. P.; Khurana, J. M. *J. Am. Chem. Soc.* **1985**, *107*, 5804–5805.